Implications of GPS-derived displacement, strain and stress rates on the 2003 Miyagi-Hokubu earthquakes

2003 Miyagi-Hokubu (Japonya) depremleri için GPS'ten elde edilen yer değiştirme, birim deformasyon ve gerilme hızlarının değerlendirilmesi

Ömer AYDAN

Tokai University, Department of Marine Civil Engineering, Shizuoka, JAPAN

ABSTRACT

Earthquake prediction has been an important field of research for years and some earthquake prediction projects such as the Tokai Earthquake Prediction Project in Japan and the Parkfield Earthquake Prediction Project in USA have been recently undertaken to progress on short-term prediction. As also shown by the author, the stress rates derived from the GPS deformation rates can be effectively used to locate the areas with high seismic risk. Furthermore, daily variations of derived strain-stress rates from dense GPS networks in Japan and USA may provide a high quality data to understand the behaviour of the earth's crust preceding earthquakes and also to predict the occurrence time of earthquakes. In this study, the method proposed by Aydan (2000) is applied to the daily GPS measurements in the northern part of Miyagi prefecture during the period between 1998 and 2003. Although the responses of deformation velocities of stations obtained from the GPS are not generally consistent with the plate tectonics model of the region, the regional strain and stress rates are in accordance with those expected from the faulting mechanism of the earthquakes. It is shown that the mean, maximum shear and disturbing stress rates can be quite useful for identifying the areas with high seismic risk in addition to tilting strains and associated stresses obtained in this article. They may be further useful for near future (in the order of months) earthquake prediction. However, they can not be used for the very near future (of the order of several hours to days) predictions unless the precision of measurements is substantially improved.

Key Words: Earthquake prediction, faulting mechanism, finite element method, global positioning system, Miyagi-Hokubu earthquakes.

ÖZ

Deprem tahmini uzun yıllardan beri çok önemli bir araştırma alanı olup, Japonya'da Tokai Deprem Tahmini Projesi ve ABD'de Parkfield Deprem Tahmin Projesi bu amaç için yürütülen projelerin belli başlılarıdır. Yazarın daha önceki bir makalesinde (Aydan, 2000) gösterildiği gibi, GPS yerkabuğu deformasyon ölçümlerinden elde edilen birim deformasyon ve gerilme hızlarını kullanarak deprem riskinin çok yüksek olabileceği alanların saptanabileceği kanıtlanmıştır. Japonya ve ABD'de yoğun GPS ağlarından elde edilen günlük ölçümlerden birim deformasyon ve gerilim hızları deprem öncesi yerkabuğunun davranışının anlaşılması ve deprem oluş zamanının kestirimi açısından oldukça yararlı olacaktır. Bu çalışmada ise, Aydan (2000) tarafından önerilen yöntem Japonya'da Miyagi vilayetinin kuzey kısmında 1998-2003 yılları arasında alınan günlük ölçümlere uygulanmıştır. GPS ölçümlerinden elde edilen deformasyonlar, bölgesel tektonik hareketlerle uyum içerisinde olmamakla birlikte, elde edilen birim deformasyon hızları ile gerilim hızları faylanma mekanizmasından beklenenlerle uyum içerisindedir. Özellikle tanımlanan ortalama, en büyük makaslama ve kırılabilirlik gerilim hızlarının deprem riskinin yüksek olduğu alanların saptanmasında oldukça yararlı olduğu bir kez daha kanıtlanmıştır. GPS yönteminin yakın gelecekte örneğin hafta ve ay mertebesinde deprem tahmininde kullanılabilir olduğuna şüphe yoktur. Bununla birlikte, çok yakın gelecekte başka bir deyişle saat mertebesinde deprem tahminine uygulanabilir olabilmesi için ölçüm hassasiyetinin oldukça arttırılması gerekmektedir.

Anahtar Kelimeler: *Deprem tahmini, faylanma mekanizması, sonlu elemanlar yöntemi, küresel konumlama sistemi, Miyagi-Hokubu depremleri.*

Ö. Aydan
E-mail: aydan@scc.u-tokai.ac.jp

INTRODUCTION

Earthquake prediction has been an important field of research for years, that resulted some success on long-term and intermediate prediction but short-time prediction is still unpredictable. Thus, some earthquake prediction projects such as the Tokai Earthquake Project in Japan and the Parkfield Earthquake Project in USA have been recently undertaken to progress on short-term prediction. The recent Parkfield earthquake on September 28, 2004 validated the prediction methodology based on the recurrence concept.

If the stress state and the yielding characteristics of the earth's crust are known at a given time, one may be able to predict earthquakes with the help of some mechanical, numerical and instrumental tools. The stress rates derived from the GPS deformation rates can be effectively used to locate the areas with high seismic risk as proposed by Aydan et al. (2000). Thus, daily variations of derived strain-stress rates from dense continuously operating GPS networks in Japan and USA may provide a high quality data to understand the behaviour of the earth's crust preceding earthquakes.

In this study, an interpolation technique of finite element method proposed by Aydan (2000; 2003), which is briefly presented, is used to compute the strain rates and consequently stress rates in the plane tangent to the surface of the earth's crust from crustal deformations. This method is then applied to the GPS measurements in the Northern part of Miyagi Prefecture, where recently large earthquakes with a magnitude of 7.0 (May 26, 2003) and 6.2 (July 26, 2003) occurred. The stress rates for the area in the close vicinity of the epicenter of M6.2 earthquake are computed and compared with seismic activity, and their implications are discussed. In addition, the general tendency of deformation pattern obtained from the GPS measurements are discussed with that expected from the tectonic model of the prefecture.

THE METHOD FOR COMPUTING TANGENTIAL STRAIN AND STRESS RATES

The crustal strain rate components can be related to the deformation rates at an observation point (x, y, z) through the geometrical relations (i.e. Eringen, 1980) as given below:

$$\dot{\varepsilon}_{xx} = \frac{\partial \dot{u}}{\partial x}; \dot{\varepsilon}_{yy} = \frac{\partial \dot{v}}{\partial y}; \dot{\varepsilon}_{zz} = \frac{\partial \dot{w}}{\partial y}; \gamma_{xy} = \frac{\partial \dot{v}}{\partial x} +$$
$$\frac{\partial \dot{u}}{\partial y}; \gamma_{yz} = \frac{\partial \dot{w}}{\partial y} + \frac{\partial \dot{v}}{\partial z}; \dot{\gamma}_{zx} = \frac{\partial \dot{w}}{\partial x} + \frac{\partial \dot{u}}{\partial z} \qquad (1)$$

Where $\dot{u}$, $\dot{v}$ and $\dot{w}$ are displacement rates in the direction of x, y and z respectively. $\dot{\varepsilon}_{xx}$, $\dot{\varepsilon}_{yy}$ and $\dot{\varepsilon}_{zz}$ are strain rates normal to the x, y and z planes and $\dot{\gamma}_{xy}$, $\dot{\gamma}_{yz}$, $\dot{\gamma}_{zx}$ are shear strain rates. The GPS measurements can only provide the deformation rates on the earth's surface (x (EW) and y (NS) directions) and it does not give any information on deformation rates in the z direction (radial direction). Therefore, it is impossible to compute normal and shear strain rate components in the vertical (radial) direction near the earth's surface. The strain rate components in the plane tangential to the earth's surface would be $\dot{\varepsilon}_{xx}$, $\dot{\varepsilon}_{yy}$ and $\dot{\gamma}_{xy}$. Additional strain rate components $\dot{\gamma}_{yz}$ and $\dot{\gamma}_{zx}$, which would be interpreted as tilting strain rate in this study, are defined by neglecting some components in order to make the utilization of the third component of deformation rates measured by GPS as follows:

$$\dot{\gamma}_{zx} = \frac{\partial \dot{w}}{\partial x}; \dot{\gamma}_{zy} = \frac{\partial \dot{w}}{\partial \dot{y}} \qquad (2)$$

Let us assume that the GPS stations re-arranged in a manner so that a mesh is constituted similar to the ones used in the finite element method. Figure 1 illustrates a simple case for triangular elements. Using the interpolation technique in the finite element method, the displacement in a typical element may be given in the following form for any chosen order of interpolation function:

$$\{\dot{u}\}=[N]\{\dot{U}\} \qquad (3)$$

Where $\{\dot{u}\}$, $[N]$ and $\{\dot{U}\}$ are the deformation rate vector of a given point in the element, shape function and nodal displacement vector, respectively. The order of shape function $[N]$ can be chosen depending upon the density of observation points. The use of linear interpolation functions has been already presented elsewhere (Aydan, 2000 and 2003). From equations (1), (2) and (3), one can easily show that the follo-
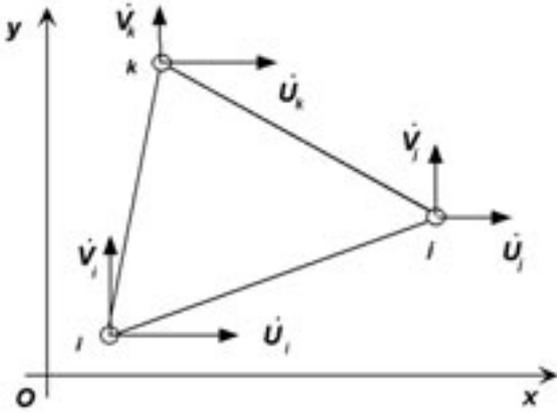
Figure 1. Coordinate system and the definition of displacement rates for a triangular element.
Şekil 1. Koordinat sistemi ve bir üçgen eleman için yer değiştirme hızlarının tanımı.

wing relation holds among the components of the strain rate tensor of a given element and displacement rates at nodal points.

$$\{\dot{\varepsilon}\}=[B]\{\dot{U}\} \qquad (4)$$

Using the strain rate tensor determined from the Eq. 4, the stress rate tensor can be computed with use of a constitutive law such as Hooke's law for elastic materials, Newton's law for viscous materials and Kelvin's law for visco-elastic materials (Aydan, 1997; Aydan and Nawrocki, 1998). In this particular study, Hooke's law is chosen and is written in the following form:

$$\begin{Bmatrix} \dot{\sigma}_{xx} \\ \dot{\sigma}_{yy} \\ \dot{\sigma}_{xy} \end{Bmatrix} = \begin{bmatrix} \lambda + 2\mu & \lambda & 0 \\ \lambda & \lambda + 2\mu & 0 \\ 0 & 0 & \mu \end{bmatrix} \begin{Bmatrix} \dot{\varepsilon}_{xx} \\ \dot{\varepsilon}_{yy} \\ \dot{\gamma}_{xy} \end{Bmatrix} \qquad (5)$$

Where λ and μ are Lame's constants, which are generally assumed to be $\lambda = \mu = 30$ GPa (Fowler, 1990). It should be noted that the stress and strain rates in Eq. (5) are for the plane tangential to the earth's surface. From the computed strain rate and stress rates, principal strain and stress rates and their orientations may be easily computed as an eigen value problem.

To identify the locations of earthquakes, one has to compare the stress state in the earth's crust at a given time with the yield criterion of the crust. The stress state is the sum of the

stress at the start of GPS measurement and the increment from GPS-derived stress rate given as:

$$\{\sigma\} = \{\sigma\}_0 + \int_{T_0}^{t} \{\dot{\sigma}\}dt \qquad (6)$$

If the previous stress $\{\sigma\}_0$ is not known, a comparison for the identification of location of the earthquake can not be done. The previous stress state of the earth's crust is generally unknown. Therefore, Aydan et al. (2000) proposed the use of maximum shear stress rate, mean stress rate and disturbing stress for identifying the potential locations of earthquakes. The maximum shear stress rate, mean stress rate and disturbing stress rate are defined below:

$$\dot{\tau}_{max} = \frac{\dot{\sigma}_1 - \dot{\sigma}_3}{2}; \sigma_m = \frac{\dot{\sigma}_1 + \dot{\sigma}_3}{2}; \tau_d = |\dot{\tau}_{max}| + \beta\dot{\sigma}_m \qquad (7)$$

Where β may be regarded as a friction coefficient. It should be noted that one (vertical) of the principal stress rates is neglected in the above equation since it can not be determined from GPS measurements. The concentration locations of these quantities may be interpreted as the likely locations of the earthquakes as they imply the increase in disturbing stress. If the mean stress has a tensile character and its value increases, it simply implies the reduction of resistance of the crust.

GPS NETWORK

The GPS network of Japan, called GEONET, is probably the most extensive network in the world and is run by Japan Geographical Survey Institute. In this study, the number of stations was chosen as 6 and the area was divided into 5 elements as shown in Figure 2. The elements are denoted as MIY_WAK_YAM, WAK_ONA_YAM, ONA_OSH_YAM, OSH_RIF_YAM and RIF_MIY_YAM with the use of first three letters of the GPS stations in clock-wise. Yamoto station is the nearest station to the epicenter of the July 26, 2003 earthquake. The area chosen may be of great interest to understand the near field displacement and stress rate variations in the close vicinity of the epicentres of earthquakes.
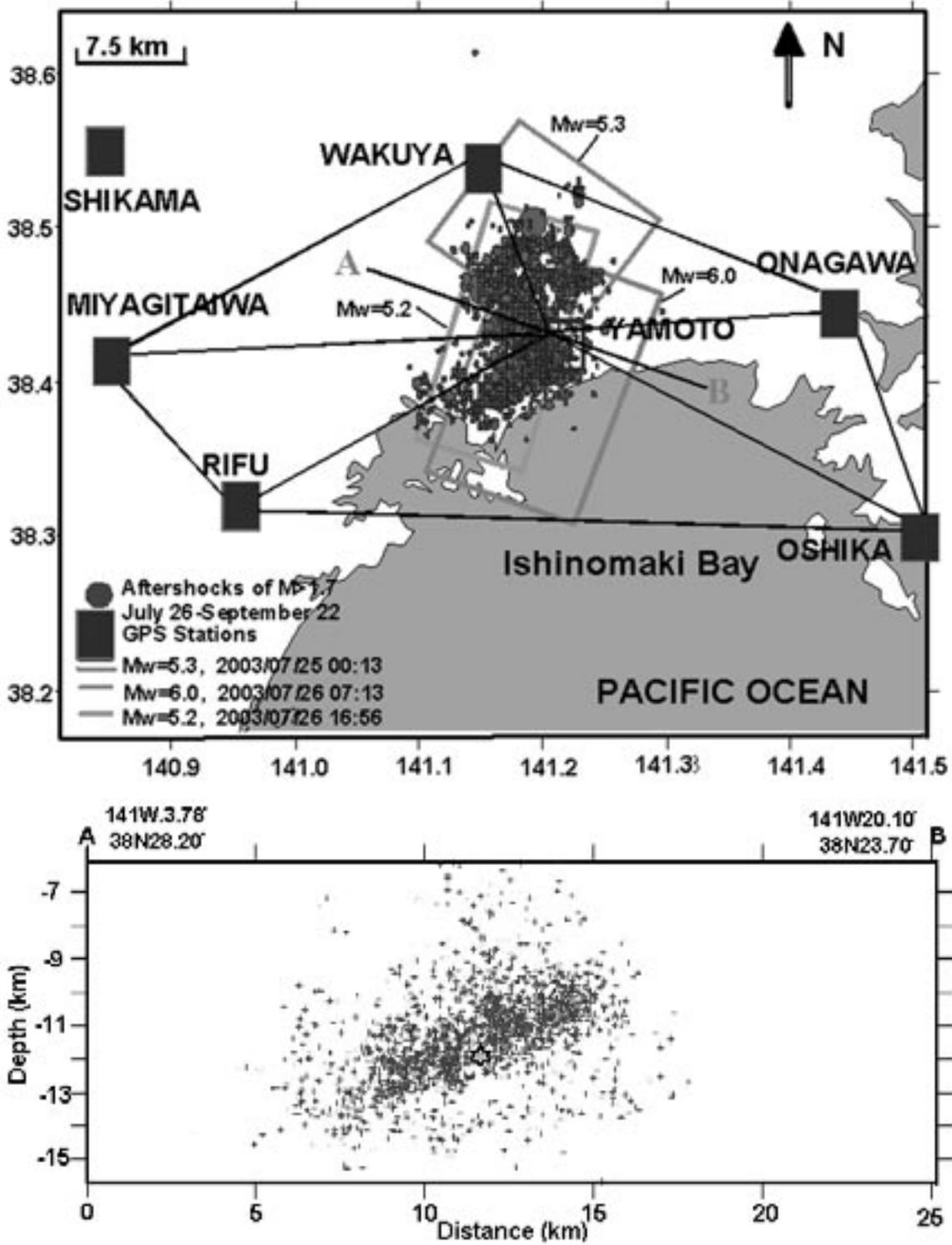
Figure 2. Seismicity map of the Nahanni fault zone for aftershocks with M>1.7 between July 26, 2003 and September 22, 2003 (GPS stations and configuration of GPS mesh and a cross-section for aftershocks through the A-B) (after Öncel and Aydan, 2003).

Şekil 2. Eylül 22, 2002 ile Temmuz 26, 2003 tarihleri arasında M>1.7'den büyük artçı depremlerin dağılımı (GPS istasyonları ve kullanılan GPS ağı ve A-B dorultusu boyunca artçıların izdüşümü) (Öncel ve Aydan 2003'ten).

CHARACTERISTICS OF THE MIYAGI EARTHQUAKE OF JULY 26, 2003

A series of earthquakes occurred in the northern part of Miyagi Prefecture of Japan on July 26, 2003 and these are officially named as Miyagi-Hokubu earthquakes. Table 1 gives the parameters of fault planes for largest foreshock and aftershock of the July 26 event. Figure 3 shows the faulting mechanism obtained by NI-ED and the normalised principal stresses associated with the earthquake inferred from the focal plane solutions using the author's method (Aydan et al., 2002). The faulting mechanism of the earthquake was caused mainly by a blind thrust fault with an almost NS strike and dipping towards west with an inclination of 30°- 45° The maximum horizontal stress acts in the direction of N83W and the least principal stress is almost vertical. The earthquakes with magnitudes of 7.0 and 5.5 occurred on May 26 and July 26, 2003, respectively, had quite similar faulting mechanisms. Fault planes for largest foreshock, aftershock and mainshock are also shown in Figure 3.

PHYSICAL BACKGROUND FOR INTERPRETATION OF MEASURED GPS RESPONSES

Some rock mechanics laboratory tests and a numerical simulation of thrust faulting are described in this section in order to have some physical background for the interpretation of variables obtained from GPS measurements. Firstly, axial stress and axial strain responses measured during a compression test on a gypsum sample from Turkey is shown in Figure 4 (Aydan et al. 2003). The sample was subjected to a very complex loading history. The rock behaves elastically when the response is linear. However, if some fracturing starts to take place in the sample, the behaviour is no longer linear and some plastic strains occur upon unloading
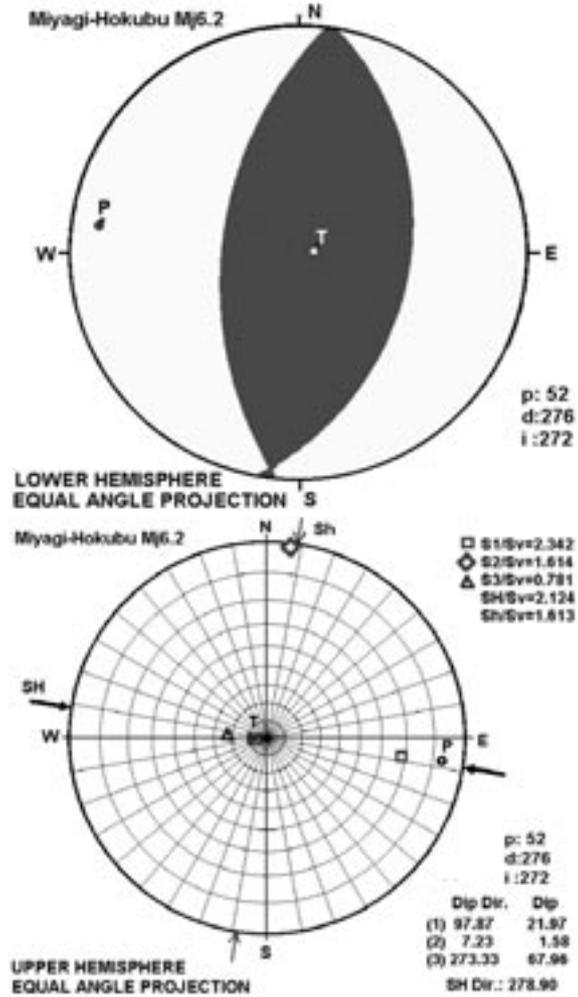

Figure 3. (a) Focal plane solution of July 26 Mj6.2 earthquake and (b) its associated stress field.
Şekil 3. (a) Temmuz 26 Mj6.2 depreminin faylanma mekanizması ve (b) ilişkin gerilme ortamı.

as noted in the figure. When rock approaches to failure, the axial strain starts to increase very rapidly.

Next, an experimental result for the response of a tuff sample subjected to a uniaxial compressi-

Table 1. Orientation of fault planes and model rupture parameters.
Çizelge 1. Fay düzlemlerinin eğimi, eğim yönü ve deprem parametreleri.

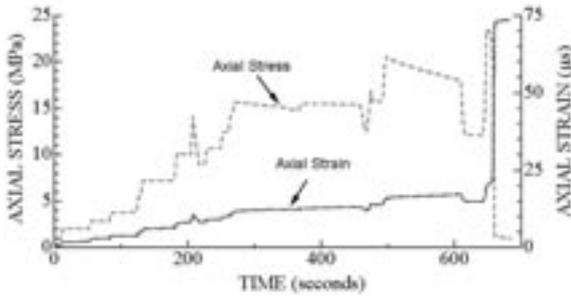| Event	Strike	Dip	Rake	L (km)	W (km)	M0 (xE17) N-m	Fault model reference	Location degree
7/25/2003	197	49	86	18	12	1.2	ERI	38.43N/141.17E
7/26/2003	201	42	102	18	15	14	ERI	38.40N/141.20E
7/26/2003	126	27	112	12	15	0.71	ERI	38.50N/141.20E

Figure 4. Mechanical responses of gypsum rock sample during uniaxial compression.
Şekil 4. Türkiye'den bir jips örneğinin tek eksenli sıkışma deneyi sırasındaki mekanik davranışı.

ve creep loading is shown in Figure 5 (Aydan et al., 1999). As seen in the figure, the axial strain shows an accelerating creep response and the rock sample fails following the linear creep stage. As noted in the results of the previous and this experiments, the failure is always associated with an accelerating strain or deformation response.

It is also known that the stick-slip tests have some relevance to the behaviour of earthquake faults (Jaeger and Cook, 1979). Figure 6a shows an example of a stick-slip experiment on a saw-cut surface of Ryukyu limestone blocks from Japan (Tokashiki and Aydan, 2003). It is of great interest that the stick-phase of deformation exhibits a linear deformation response and the slip behaviour is distinguished with a sharp offset of deformation. Figure 6b shows a close-up view of the response during the second slip event. As
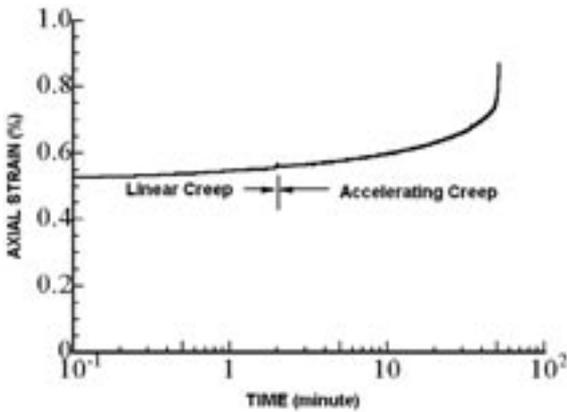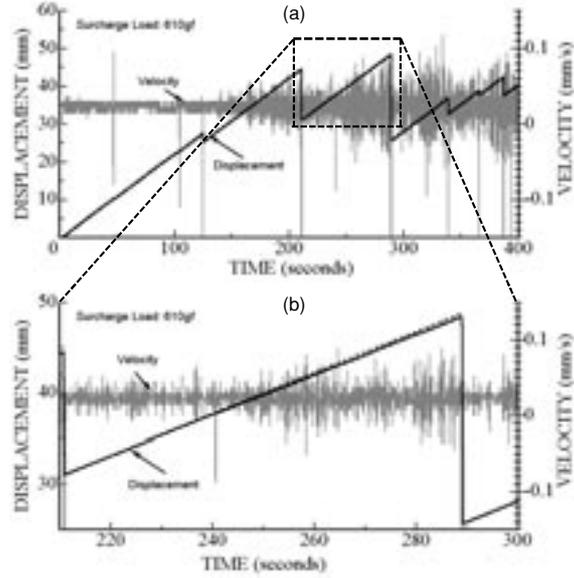

Figure 6. Stick-slip response of saw-cut Ryukyu (Japan) limestone blocks.
Şekil 6. Ryukyu (Japonya) kireçtaşı bloklarının kesik arayüzeyinin yapışma-kayma davranışı.

noted from the figure, the linear deformation response in stick phase tends to deviate from the linear behaviour before the slip. In other words, the velocity was no longer constant and it fluctuated before the slip took place.

As the faulting mechanisms of the Miyagi earthquakes were mainly thrust faulting, numerical simulations carried out by Aydan (2002) on the deformation responses of the faults during thrust faulting using Discrete Finite Element Method (DFEM) are referred herein to have some ideas on the expected ground deformations before, during and after the earthquake. Figure 7 shows the boundary conditions imposed on
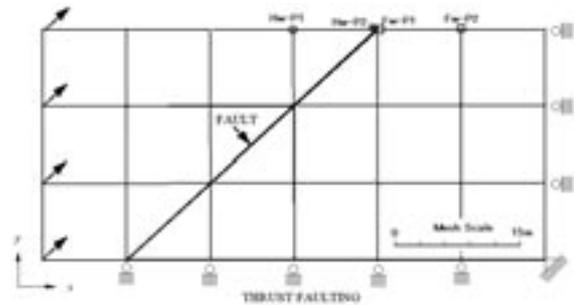

Figure 5. Creep response of Ürgüp (Turkey) tuff.
Şekil 5. Ürgüp (Türkiye) tüfünün krip davranışı.

Figure 7. Finite element mesh used in DFEM analysis.
Şekil 7. DFEM analizinde kullanılan sonlu elemanlar ağı ve sınır koşulları.

the numerical faulting model. The numerical fault model was subjected to forced displacements of 100 mm horizontally and vertically along the vertical and horizontal boundaries of hanging wall side of the fault plane. In the same figure, four control points on the ground surface are selected. Figure 8 shows deformed configurations for different steps of the computation, which may be viewed as a fictious time step. The first step corresponds the elastic response of the model. As noted from the figure, the ground surface is tilted and the whole body is compressed horizontally. However, once the fault starts to rupture near the lower boundary, the compressed footwall of the fault is relaxed and relative sliding starts to take place along the fault. Figure 9 shows the displacement responses of points on the hanging wall and footwalls following the initial elastic displacement. The elas-
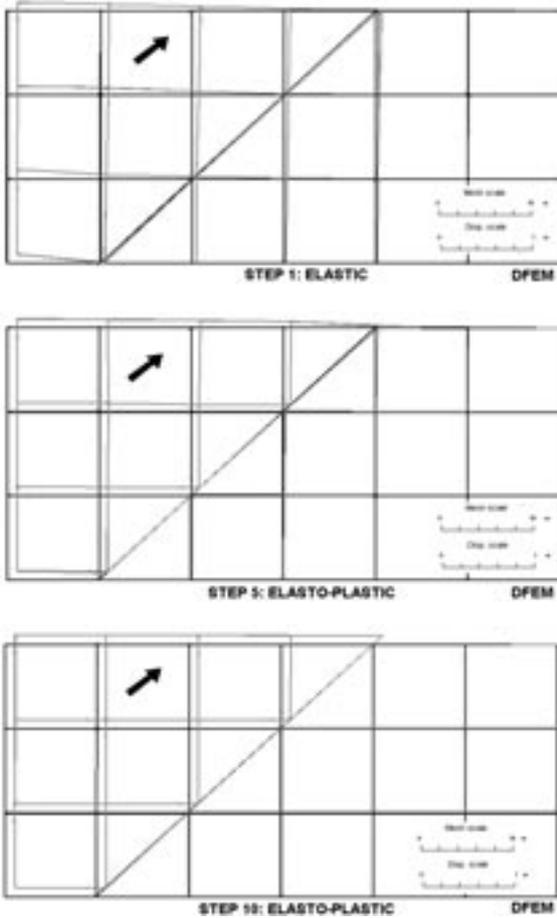

Figure 8. Deformed configurations during various computation steps.
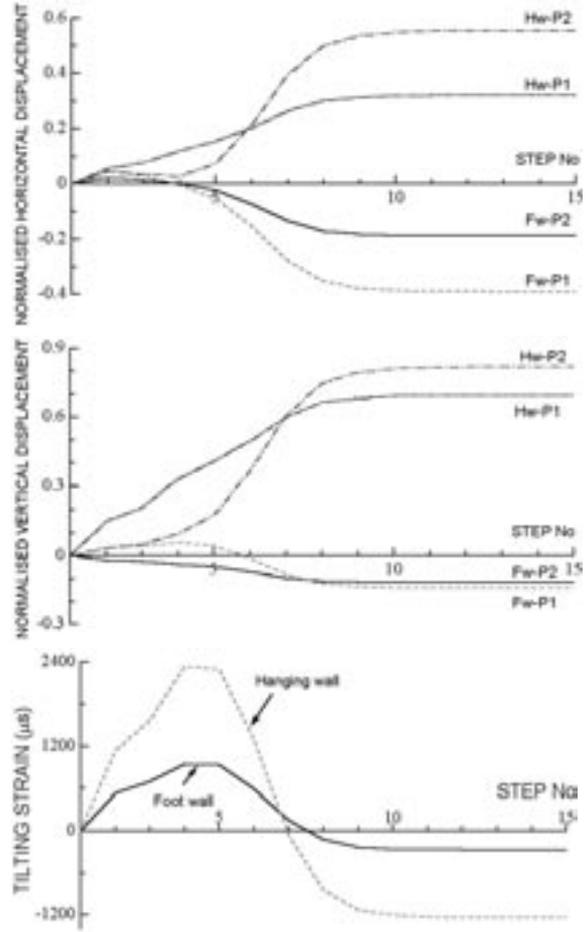Şekil 8. Değişik hesaplama aşamalarında yerdeğiştirme durumları.

Figure 9. Responses of control points on the footwall, hanging wall and tilting strain.
Şekil 9. Taban ve tavan bloklarındaki kontrol noktalarının yerdeğiştirme davranışı ve eğilme birim deformasyonu.

tic displacement is subtracted from the displacement responses, and the resulting displacement is normalised by the forced displacement at the boundary. The normalised horizontal displacements of control points on the footwall decrease, while those of control points on the hanging wall increase as the fracture propagation progresses. Similar responses are also observed for the normalised vertical displacement of control points. The variation in displacements of the control points far from the fault plane is gradual while those of control points nearby the fault plane are sharp during the propagation of the fault. The tilting strain perpendicular to the strike of the fault decreases gradually as the compressed body is released from the forced displacement field.

GPS MEASUREMENTS AND THEIR EVALUATION

Displacement Rates

The expected deformation pattern for the faulting mechanism from the previous two-dimensional analysis implies that there should be contraction along perpendicular (EW direction) to the strike of the fault and the extension parallel to the fault strike (NS direction) due to Poisson effect. As for the vertical motion, the east side of the fault (denoted B in Figure 2) should be moving downward while the motion of its west side should be upward.
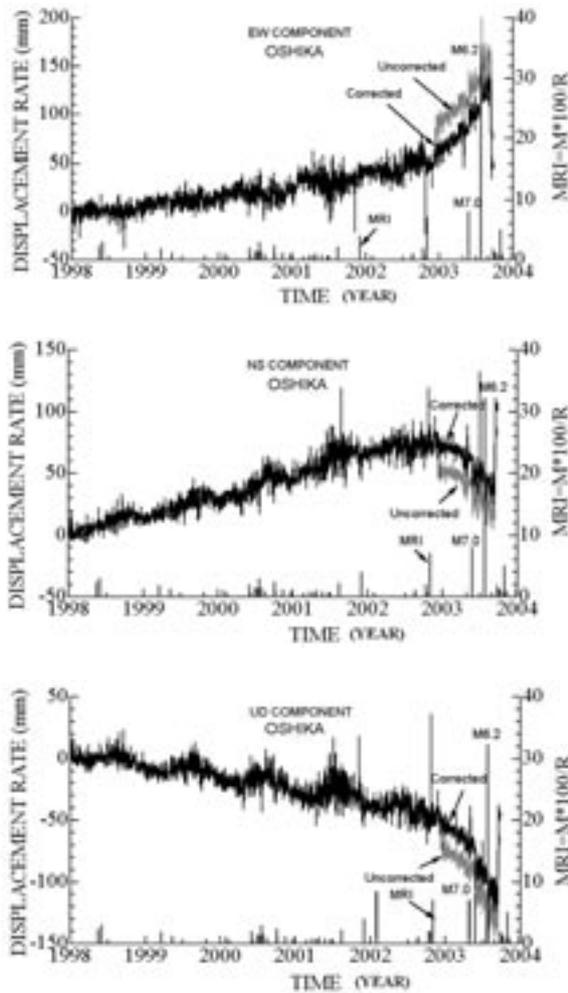

Figure 10. Uncorrected and corrected time series of displacement rates of Oshika GPS station.
Şekil 10. Oshika GPS istasyonunda düzeltilmemiş ve düzeltilmiş yerdeğiştirme miktarının zamana bağlı değişimi.

Figure 10 shows the displacement rates for Oshika GPS station versus time. The displacement rates presented in this study are obtained by subtracting the global coordinates of GPS stations with respect to those on the 1st january of 1998. The right vertical axis is defined as MRI $=M \times 100 / R$, in which M is magnitude, R is hypocenter distance (km). The index MRI may be an indicator of the effect of earthquakes on the region. In Figure 10, there are two time series plots of the deformation rates; one is for an uncorrected plot and the other is an corrected plot. The offsets in displacement rates of all stations were observed in December 2002. Nevertheless, there was no significant earthquake in the region within a radius of 500 km or worldwide during that period. If the measured GPS data are reliable, these should be corresponding to some silent crustal movements. However, the author have recently found out that these offsets were due to the antenna replacement of the GPS stations in the region in December 2002. Therefore, some corrections were done on the time series plot of the displacement rates for all GPS stations by taking into account the general trend of before and after the antenna replacement.

Figure 11 shows the time series plots of the corrected displacement rates for all GPS stations. Rifu and Miyagi-Taiwa stations on the hanging-wall of the causative fault while Oshika and Onagawa GPS stations are on its foot-wall block. Wakuya GPS station is almost at the north tip of the causative fault, while Yamoto GPS station is just on the fault. It is noted that there are some sinusoidal year-long fluctuations of the displacement rates. These fluctuations are due to the deformation of the earth due to its motion around the sun. The displacement rates of Yamoto and Oshika stations are the most striking ones and these stations move in the direction of SE after the beginning of 2003 while they subside as expected from the fault deformation before the release of stored mechanical energy by the earthquake. On the other hand, the rest of other GPS stations moves NW while they are uplifted. The deformation responses after the beginning of 2003 are similar to those in the accelerating stage of creep tests as discussed in the previous section.
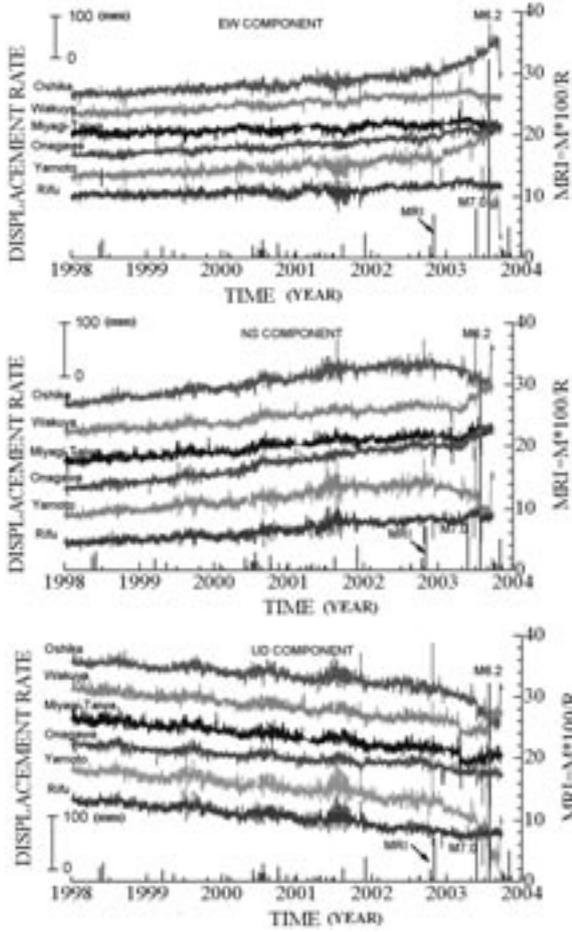
Figure 11. Corrected time series of displacement rates of all GPS stations.
Şekil 11. Bütün GPS istasyonunda düzeltilmiş yerdeğiştirme miktarının zamana bağlı değişimi.

Figure 12. Time series of minimum, maximum principal and maximum shear strain rates of GPS elements.
Şekil 12. Bütün GPS elemanlarının en büyük, en küçük asal ve en büyük makaslama birim deformasyonlarının zamana bağlı değişimi.

Strain Rates

The interpretation of deformation velocity components of GPS stations becomes meaningless when they are considered individually. Therefore, the utilization of strain and stress rates is more meaningful as they are the indicators of the distribution of regional straining. The sign convention for strain rate tensor follows that of the continuum mechanics. Therefore, maximum principal stress rate has either an extensional character or the least compressive strain while minimum principal strain rate is vice versa. Figure 12 shows the maximum (tensile), minimum (compression) and maximum shear strains of each GPS element with time. It is of great interest that the year-long sinusoidal fluctuations observed in displacement responses almost di-
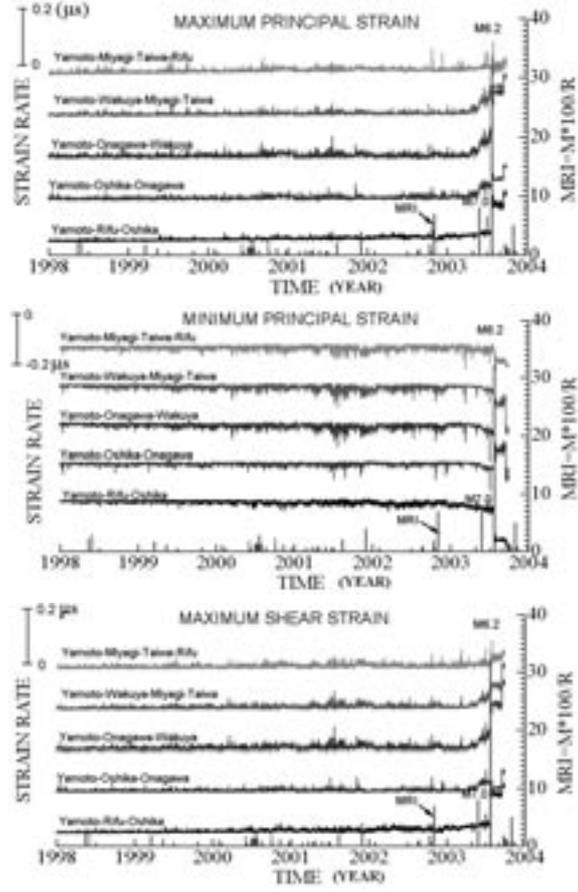
sappeared in the computed strain rates. In other words, if the strain rate concept is used, there is no need to consider the displacement component of the earth's crust due to the year-long motion of the earth around the sun.

The strain rate components of Yamoto-Rifu-Oshika element indicates a visible linear strain rate variation with time while strain variations of other GPS elements are not distinct at all. The strain rate high strain variations of Yamoto-Rifu-Oshika element become more apparent in October 2002. The epicenter of the main shock was located within this element. However, the strain rate components of the elements of Yamoto-Oshika-Onagawa, Yamoto-Onagawa-Wakuya and Yamoto–Wakuya-Miyagi-Taiwa started to change remarkably at the beginning of

May, 2003 and after M7.0 of Kinkazan earthquake on May 26, 2003, the strain rates of these element became greater with time. The high rate of variations after the M7.0 earthquake resulted in a series of earthquakes on July 26, 2003, called Miyagi-Hokubu earthquakes. As noted from the figure, extensional strain rates are larger than compressive strain rates. It is also noted that the maximum shear strain rates may be a good indicator of regional straining.

Figure 13 shows the tilting strain rates for all GPS elements. Since the element of Yamoto-Rifu-Oshika spans over both sides of the fault, the tilting strain components of this element are smaller than those of other elements. The tilting strain components of Yamoto-Onagawa-Wakuya and Yamoto-Wakuya-Miyagi-Taiwa are greater than those of other GPS elements. All strain rate components resemble accelerating creep strain responses particularly after the beginning of 2003. The strain rates are particularly accelerated following the M7.0 Kinkazan earthquake.

Stress Rates

First maximum and minimum principal stress rates and shear stress rate associated with tilting
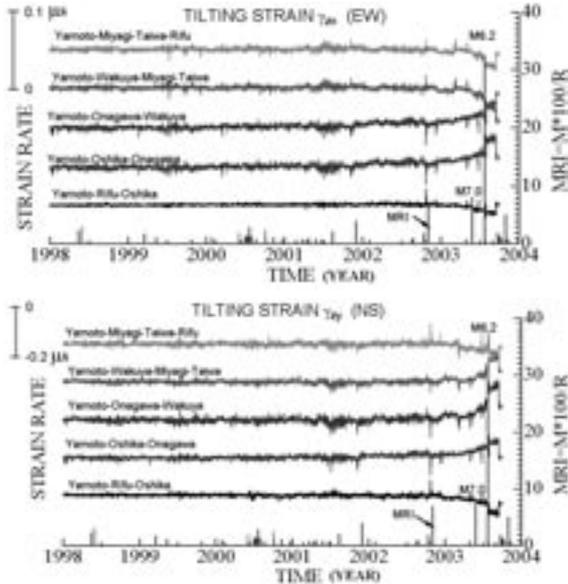

Figure 13. Time series of tilting strain rates of GPS elements.
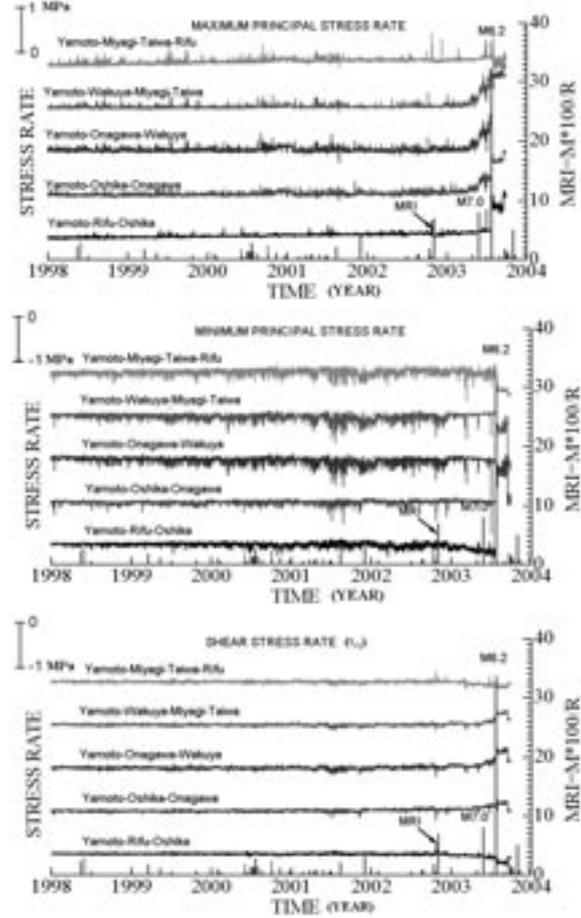*Şekil 13. Eğilme birim deformasyonlarının zamana bağlı değişimi.*

Figure 14. Time series of maximum, minimum principal stresses and shear stress associated with tilting strain rates of GPS elements.
Şekil 14. En büyük, en küçük asal ve eğilme makaslama gerilmelerinin zamana bağlı değişimi.

strains are shown in Figure 14. The sign convention for stress rate tensor follows that of the continuum mechanics. Therefore, maximum principal stress rate has either a tensile character or the least compressive stress while minimum principal stress rate is vice versa. The largest compressive stress rates occur almost in EW direction while the least compressive or tensile stress rates are aligned along NS direction. It is of great interest that a regional unloading occur before the earthquake since the maximum principal stress rate, which is of tensile character, increases while the minimum principal stress rate is almost constant. The time of remarkable variations are the same those stated for strain rates. The shear stress rates associated with tilting strains also indicate remarkable changes after the beginning of 2003.

Aydan et al. (2000) found better correlations among the stress rates given by Eq. (7) and earthquake occurrences. The characters of mean, maximum shear and disturbing stress rates have certain meanings for the interpretation of faulting mechanism and seismic risk of the regions. The mean, maximum and disturbing stress rates are computed and results are shown in Figure 15, using the stress rate definitions given by Eq. (7).

The stress rate components of Yamoto-Rifu-Oshika element indicates that remarkable stress variations started in October 2002 as noted in the previous sub-sections. However, the strain rate components of the elements of Yamoto-Oshika-Onagawa, Yamoto-Onagawa-Wakuya and Yamoto-Wakuya-Miyagi-Taiwa started to change remarkably at the beginning of May, 2003 about 1 month before the M7.0 Kinkazan earthquake that occurred on May 26,
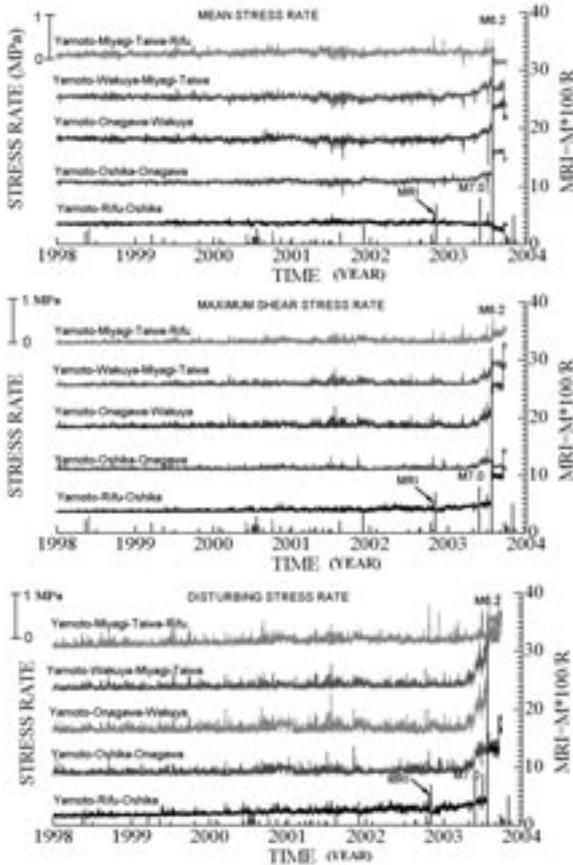
2003. The high rate of variations continued after the M7.0 earthquake and resulted in July 26, 2003 Miyagi-Hokubu earthquakes. As noted from the figure, the variations of disturbing stress rates are greater than those of mean and maximum shear stress rates. This may indicate that the disturbing stress rate may be a good indicator of regional stress variations and precursors of following earthquakes.

As noted from Figure 15, large changes in mean, maximum shear and disturbing stress rates are observed following the M7.0 earthquake. Very large variations observed in computed stress rate components stations of all elements was first observed on February 26, May 26 and June 26. These events almost correspond to the moon phase and moon distance relative to the Earth as seen in Figure 16.

CONCLUSIONS

In this study, the principles of a method for the computation of strain and stress rates in a plane tangential to the earth's surface from GPS measurements are briefly presented. This method is then applied to the GPS measurements in the northern part of Miyagi Prefecture between 1998 and 2003. Although the response of deformation rates of the stations obtained from GPS measurements are not generally consistent with the plate tectonics model of the region, the regional strain and stress rates are in accordance with those expected from the faulting mechanism of the earthquakes.

As seen in the previous applications to the GPS measurement in Turkey (Aydan et al. 2000, Aydan 2003), the mean, maximum shear and disturbing stress rates can be quite useful for iden-
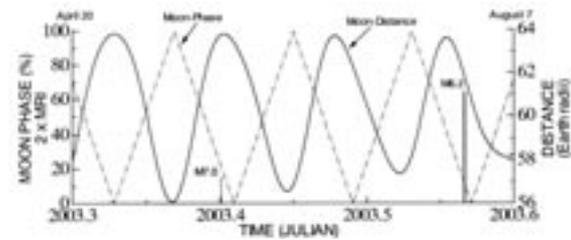

Figure 15. Time series of mean, maximum shear and disturbing stress rates of GPS elements.
Şekil 15. Ortalama, en büyük ve eğilme makaslama gerilmelerinin zamana bağlı değişimi.

Figure 16. The variation of moon-distance and moon-phase between April 20 and August 7, 2003.
Şekil 16. 2003 yılında Nisan 20 ile Ağustos 7 arasında ayın uzaklığı ve durum değişimi.

tifying the areas with a high seismic risk. They may be further useful for near future (in the order of months) earthquake prediction. However, they can not be used for very near future predictions, say, in the order of several hours to days unless their sensitivity of measurements is substantially improved. Furthermore, the changing antenna and some artificial causes such as the releasing correct information on the exact positions of satellites operated by USA (i.e. offsets during Iraq war) may cause some undesirable offsets. If the earthquake predictions utilize GPS measurements, such offsets may result in false alerts.

ACKNOWLEDGEMENT

REFERENCES

Aydan, Ö., 1997. Dynamic uniaxial response of rock specimens with rate-dependent characteristics. Proceedings of the South African Rock Engineering Symposium, Johannesburg, SARES'97, 322-331.

Aydan, Ö., 2000. Annual strain rate and stress rate distributions of Turkey from GPS Measurements, Yerbilimleri, 22, 21-32.

Aydan, Ö., 2002. Actual observations and numerical simulations of surface fault ruptures and their effects on engineering structures. 8th Workshop on Earthquake Resistant Design of Lifeline Facilities and Countermeasures against Liquefaction, Tokyo, Japan.

Aydan, Ö., 2003. The earthquake prediction and earthquake risk in Turkey and the applicability of global positioning system (GPS) for these purposes. Turkish Earthquake Foundation, TDV/KT 024-87, 1-73 (in Turkish).

Aydan, Ö., and Nawrocki, P., 1998. Rate-dependent deformability and strength characteristics of rocks. Proceeding of the Inernational Symposium on the Geotechnics of Hard Soils-Soft Rocks, Napoli, 1, 403-411.

Aydan, Ö., Ulusay, R Yüzer, E., Erdoğan, M., and Kawamoto, T., 1999. A research on the living environment of Derinkuyu Underground City, Central Turkey. (MONBUSHO Research Project No: 09044154) (in Japanese).

Aydan, Ö., Kumsar, H., and Ulusay, R., 2000. The implications of crustal strain-stress rate variations computed from GPS measurements on the earthquake potential of Turkey. International Conference of GIS on Earth Science and Applications. ICGESA-'2000, Menemen (on CD).

Aydan, Ö., Kumsar, H and Ulusay, R., 2002. How to infer the possible mechanism and characteristics of earthquakes from the striations and ground surface traces of existing faults, JSCE, Earthquake and Structural Engineering/Earthquake Engineering, 19 (2), 199-208.

Aydan, Ö., Tokashiki, N., Ito, T., Akagi, T., Ulusay, R., and Bilgin, H. A., 2003. An experimental study on the electrical potential of non-piezoelevtrik geomaterials during fracturing and sliding, Proceeding of the 9th ISRM Congress, South Africa, 73-78.

Eringen, A.C., 1980. Mechanics of Continua, R.E. Krieger Pub. Co., New York.

Fowler, C.M.R., 1990. The solid earth - An introduction to Global Geophysics, Cambridge University Press, Cambridge.

Jaeger, J.C and Cook, N.G.W., 1979. Fundamentals of Rock Mechanics, 3rd Edition, 593 pp. Chapman and Hall, London.

Öncel, A., and Aydan, Ö., 2003. Variations in GPS-derived displacement and stresses during the 2003 Miyagi earthquakes. Proceeding of the International Colloquium on Instrumentation and Monitoring of Landslides and earthquakes in Japan and Turkey, Koriyama, (H. Tano and Ö. Aydan (eds.)), 81-90.

Tokashiki, N., and Aydan, Ö., 2003. Characteristics of Ryukyu Limestone and its utilization as a building stone in historical and modern structures. Proceeding of the International Symposium on Industrial Minerals and Building Stones, İstanbul, 311-318.